Formation and Variability of a Northerly ITCZ in a Hybrid Coupled AGCM: Continental Forcing and Oceanic–Atmospheric Feedback*

SHANG-PING XIE AND KAORI SAITO+

Graduate School of Environmental Earth Science, Hokkaido University, Hokkaido, Japan

(Manuscript received 17 December 1999, in final form 10 May 2000)

ABSTRACT

Despite the equatorial symmetry of the annual-mean insolation, the intertropical convergence zone (ITCZ) and the collocated band of high sea surface temperature (SST) assume perennial northern latitudes over the eastern Pacific and Atlantic. An atmospheric general circulation model is coupled with an intermediate ocean model to study continental forcing and oceanic–atmospheric interaction that act to break the equatorial symmetry. The model reaches a statistically symmetric mean state under perfectly symmetric conditions with the continental coasts running along meridians. When a bulge of landmass is added to the eastern continent north of the equator, it initiates a coupled ocean–atmosphere wave front that propagates westward across the ocean basin, cooling the ocean surface and suppressing deep convection on and south of the equator. As a result, the ITCZ shifts into the Northern Hemisphere. In contrast to this basinwide response, little latitudinal asymmetry develops in the coupled model when the same land bulge is moved to the western continent, with the ITCZ staying on the equator. These model experiments demonstrate that the meridional structure of the oceanic ITCZ is largely determined by the continental geometry in the east, lending support to a westward control hypothesis based on simple linear wave dynamics.

Under steady solar forcing, the model ITCZ displays substantial interannual variability in both intensity and latitude. A coherent interhemispheric SST pattern with opposing polarities is found to be associated with this ITCZ variability. Various oceanic–atmospheric feedback mechanisms involved in the formation and variability of the ITCZ are examined.

1. Introduction

The tropical climate displays peculiar perennial features inexplicable from the solar radiation forcing function. Most notably, deep convective activity and the associated rainfall over the eastern Pacific and the Atlantic reach a local minimum at the equator and are displaced into the Northern Hemisphere (Mitchell and Wallace 1992 among others), despite an annual-mean insolation distribution at the top of the atmosphere that has a local maximum at and is nearly symmetric with respective to the equator. Ocean–atmosphere interaction is responsible for such inconsistency between the solar forcing and climatic response because as the first approximation, tropical rainfall is determined by sea surface temperature (SST) while SST is in turn affected by rainfall distribution via surface winds. Specifically, equatorial convection is suppressed by cooling associated with equatorial upwelling, a direct consequence of the development of the Walker circulation/cold tongue complex involving the Bjerknes (1969) feedback (Dijkstra and Neelin 1995; Sun and Liu 1996). Other types of interactions involving wind–evaporation–SST (WES; Xie and Philander 1994), upwelling–SST (Chang and Philander 1994), and stratus cloud–SST (Philander et al. 1996) feedbacks are proposed as mechanisms that break the equatorial symmetry set by solar radiation. Li (1997) examined the relative importance of these feedback mechanisms in maintaining the equatorial asymmetric SST field in a coupled model.

How the coupled system develops an equatorial asymmetric climate that favors a Northern Hemisphere (NH) intertropical convergence zone (ITCZ) under symmetric solar forcing is a focus of this study. While pushing the ITCZ away from the equator, the above mentioned ocean–atmospheric feedbacks do not favor either hemisphere. While the land–sea distribution appears responsible for displacing the Pacific and Atlantic ITCZs into the NH, it is still controversial which continental features and how they do so. Without some ad hoc flux

* International Pacific Research Center Contribution Number 69 and School of Ocean and Earth Science and Technology Contribution Number 5307.

+ Current affiliation: Kyodo News Agency, Chuo-Ku, Kobe, Japan.

Corresponding author address: Dr. Shang-Ping Xie, International Pacific Research Center/School of Ocean and Earth Science and Technology, University of Hawaii at Manoa, 2525 Correa Road, Honolulu, HI 96822.
E-mail: xie@soest.hawaii.edu

adjustment schemes, many coupled GCMs (CGCMs) suffer the double-ITCZ syndrome, with the ITCZ moving back and forth across the equator following the seasonal march of the Sun (Mechoso et al. 1995; Li and Hogan 1999). Such cross-equatorial seasonal march leaves an unrealistic double ITCZ in the annual-mean rainfall. In the real Pacific, a double ITCZ appears only briefly in March and April, with the ITCZ confined to the north of the equator for the rest of a year. The configuration of the ITCZ in coupled models is further sensitive to the choice of physical parameterization schemes (Terray 1998).

Several recent CGCM studies of the Pacific ITCZ focus on continental features on the Americas. Philander et al. (1996) show that the tilt of the west coast of the Americas can force the Pacific ITCZ to move northward, particularly when the stratus–SST feedback is enhanced in the model. Other CGCM experiments confirm this result and show that an enhancement of stratus clouds off the Peruvian coast can cause a basinwide northward displacement of the ITCZ in the steady state (Ma et al. 1996; Kimoto and Shen 1997; Iizuka et al. 1998). Whereas the responsible mechanisms remain to be clarified in the CGCMs, this sensitivity to forcing in the east appears to be due to the fact that antisymmetric waves in both the ocean and atmosphere can propagate only westward under the longwave approximation. In an intermediate models, Xie (1996) shows that a coupled WES wave front excited on the eastern boundary travels westward across the basin, displacing the ITCZ northward.

The above studies lead to a westward control hypothesis, implying that the eastern continent is more important than the western one in setting up the ITCZ's latitudinal asymmetry. Here we will extend Xie's (1996) work by coupling an atmospheric GCM (AGCM) with an intermediate ocean model. Such a hybrid coupled AGCM (HaGCM) fills a gap between intermediate models and highly complex coupled GCMs, two extreme classes of models previous studies are based on. The Matsuno (1966)–Gill (1980; MG hereinafter) model Xie used differs from an AGCM/real atmosphere in a number of important ways that affect ocean–atmospheric feedbacks. First, the MG model computes the time-mean surface wind velocity, but variable winds are important for evaporation at the ITCZ (Esbensen and McPhaden 1996). A northerly ITCZ induces southerly cross-equatorial winds that reduce mean wind velocity under the Coriolis force, a positive feedback acting to weaken surface evaporation and maintain high SST. On the other hand, convective activity as manifested by traveling cloud clusters within the ITCZ causes large wind variability, a negative feedback not included in the MG model. Figure 1 shows such an example: the monthly mean wind velocity ($\mathbf{U}$) at the ITCZ is vanishingly small, but the mean scalar wind speed ($\overline{|\mathbf{U}|}$) remains high, exceeding the speed of mean vector wind by 4 m s^{-1}. Here the overbar denotes the time mean. Second,

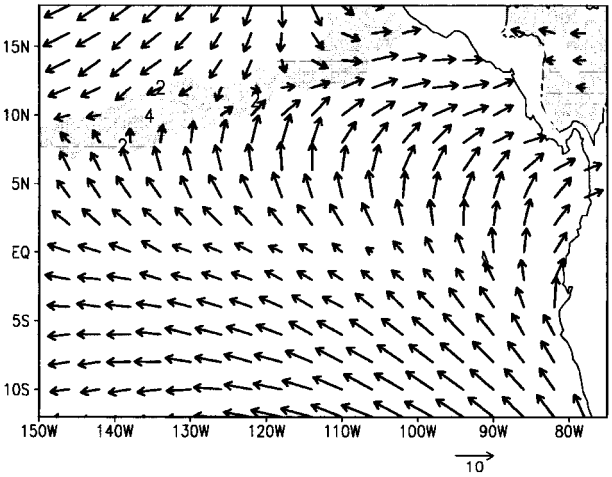

FIG. 1. Monthly mean wind velocity averaged for Sep 1999 (vectors) and the difference between the speeds of mean scalar and vector wind ($\overline{|\mathbf{U}|} - |\overline{\mathbf{U}}|$ in contours; shade > 1 m s^{-1}). The daily, high-resolution QuikSCAT satellite wind data (Liu et al. 2000) are used.

enhanced deep clouds at the NH ITCZ is a negative feedback to local SST whereas increased low clouds on the other side of the equator is a positive one. Third, cross-equatorial winds are weak in the MG model, underestimating the upwelling–SST feedback. Four, whereas the MG model simulates the equatorial zonal wind quite well (e.g., Zebiak 1982), its skill in simulating the off-equatorial wind, central to the WES feedback, is still under intense debate. The wind response in an AGCM to equatorially antisymmetric SST can be quite different from that in the MG model (Sutton et al. 2000). Finally, it remains to be seen how valid an argument based on linear equatorial wave dynamics like the westward control hypothesis is in a moist atmosphere where the interaction of the flow and heating fields is highly nonlinear.

The present study tests the westward control mechanism in the HaGCM that contains not only the WES but also other positive and negative feedbacks as mentioned above. We will examine how a continental asymmetry sets up an asymmetric circulation over the ocean and how ocean–atmosphere interaction then helps establish the basin-scale asymmetry in response. A key question is whether the model ITCZ is more sensitive to a perturbation on the eastern than on the western continent. Three idealized experiments are conducted that are designed to yield a straightforward answer to the question. We will first run the HaGCM under a perfectly equatorial symmetric land–sea distribution. Then, we add an asymmetric perturbation onto the continent either to the east or to the west, and observe if there is any difference in the model response.

The Atlantic ITCZ varies its latitude on both interannual and decadal timescales, in association with a dipole SST pattern in the meridional direction [Nobre and Shukla (1996) and references therein]. Whereas the

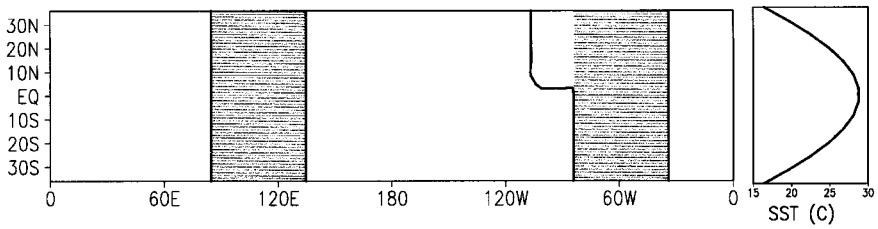

FIG. 2. Land–sea distribution (left) and meridional profile of the prescribed SST (right). The continents in the symmetric control run are shaded.

WES feedback is proposed to be a responsible mechanism (Carton et al. 1996; Chang et al. 1997; Xie 1999), it is currently under much debate whether the tropical Atlantic SST dipole is a dynamic mode of ocean–atmosphere interaction [Enfield et al. (1999) and references therein]. Attempts with AGCM simulations to evaluate the feedback of wind-induced evaporation on SST are inconclusive, with its sign varying from negative in one GCM (Sutton et al. 2000) to regionally positive within a near-equatorial zone in another (Chang et al. 2000). The ITCZ variability, which is absent in intermediate models that lack stochastic forcing, is the another focus of this study. Questions we ask are: Is there a characteristic SST pattern associated with the ITCZ variability in this HaGCM? If so, what are the ocean–atmosphere interaction mechanisms that produce this structure?

The rest of the paper is organized as follows. The next section introduces the hybrid model and its components. Section 3 describes the response of the standalone AGCM to an asymmetric continental feature. Section 4 examines the coupled response to the same continental forcing and compares it with a case when the forcing is moved to the west. Section 5 discusses temporal variability in the model, with a focus on the north–south seesaw. Section 6 concludes our study.

2. Model

This study is concerned with how a latitudinal asymmetry in land surface distribution can force asymmetries in the adjacent atmosphere and how it might trigger the interaction with the ocean that leads to basinwide asymmetries in SST and rainfall distributions. For this purpose, we couple an AGCM with an intermediate ocean model, in contrast to previous hybrid coupled models (Neelin et al. 1998) that employ ocean GCMs to better represent ocean dynamics crucial for the ENSO. The atmospheric GCM offers interactive treatment of thermal and moisture conditions of land surface as the purpose of this study requires. Built on our previous coupled studies including those with the hybrid coupled OGCMs, the intermediate complexity of our ocean component makes the model results easy to interpret and allows direct comparison with previous simple/intermediate model studies.

a. Atmospheric GCM

The AGCM is developed jointly by the University of Tokyo's Center for Climate System Research and the National Institute for Environmental Studies in Japan. It solves primitive equations of motion in spherical spectrum form. Here we use a version with a triangle truncation at zonal wavenumber 21 (T21) and 20 sigma levels in vertical. The model employs a modified Arakawa–Schubert (1974) moist convection scheme. Cloud water is predicted (Le Treut and Li 1991) and radiation is calculated according to Nakajima and Tanaka (1986). Readers are referred to Numaguti et al. (1997) and Numaguti (1999) for details of model physics and its performance.

Ground hydrology is represented by a 15-cm-deep bucket model (Manabe et al. 1965). Predicted from precipitation, evaporation, and runoff, soil moisture content in the bucket determines the ratio of actual to potential evaporation, which in turn affects the surface temperature and PBL height. Thus the soil moisture content is an important property that distinguishes land from ocean surface, and its prognostic treatment meets our purpose. The land surface is flat at the sea level, with its albedo set constant everywhere at 0.25, a value typical of grass land. Results from coupled experiments with a smaller albedo (0.11, forest) are qualitatively similar to what to be described. Albedo for ocean surface is set at 0.07. A land–sea distribution perfectly symmetric about the equator is used in the control runs: two continents are each 40° wide in longitude (90°–30°E and 80°–40°W) whereas two oceans, 140° wide in longitude, fill the basins in between (Fig. 2). SSTs are initially specified in an equatorially symmetric distribution.

To focus on the formation of the annual-mean climatology, we fix the insolation throughout the experiments at its equinox value that is symmetric about the equator. The effects of the seasonal cycle will be left for future studies. The diurnal cycle of insolation is retained in the model calculation, which has an effect on the vertical structure of the planetary boundary layer over the land surface.

b. Ocean model

The ocean component is based on the Zebiak–Cane (1987) model, where the total SST is determined by the equation:

$$\frac{\partial T}{\partial t} + u\frac{\partial T}{\partial x} + v\frac{\partial T}{\partial y} + w\frac{T - T_e}{H_e}P(w) = \frac{Q}{\rho c_p H} + \kappa\nabla^2 T. \quad (2.1)$$

Here (u, v) are surface current velocity, w is the vertical velocity at $H = 50$ m—the depth of the Ekman/mixed layer—with $P(w)$ the Heaviside function, Q is the surface heat flux into the ocean with ρ and c_p being the density and specific heat at constant pressure of sea water, respectively, and $\kappa = 2 \times 10^3$ m^2 s^{-1} is the horizontal diffusivity. Temperature of water at depth $H_e = 100$ m that is entrained into the mixed layer is a function of thermocline depth (h)

$$T_e = T_0 - \frac{\Delta T}{2}\left\{1 - \tanh\left[\frac{(h + h_0)}{H^*}\right]\right\}, \quad (2.2)$$

where $T_0 = 30$°C, $\Delta T = 16$°C, $h_0 = 30$ m and $H^* = 50$ m (Dijkstra and Neelin 1995; Xie 1998).

Near the equator where oceanic upwelling prevails, the variation of thermocline depth strongly affects SST field, being the dominant mechanism for the eastern cold tongue and interannual variability like the ENSO [see Neelin et al. (1998) for a latest review]. A few degrees off the equator, by contrast, the general Ekman downwelling shuts off this subsurface effect on SST. In fact, the thermocline shoals underneath the warm SST band collocated with the ITCZ, an h–T relationship opposite to that associated with the ENSO on the equator. Instead of upwelling and ocean wave dynamics, the adjustment through surface heat flux becomes important in determining SST. Based on these considerations, we make a further simplification of the ocean model by specifying a time-invariant thermocline depth field, $h(x, y)$. This removes the thermocline depth feedback and stabilizes the coupled ENSO mode that would otherwise give rise to large interannual variability—undesirable noise for our present purpose of studying the mean climate. The elimination of ENSO-like variability shortens the time necessary to obtain a statistically steady state and more importantly, allows a clear view of processes involved in establishing tropical climatology. The effects of interactive ocean wave dynamics will be a subject of future investigations. The thermocline depth field to be prescribed in this study is the steady-state solution to a linear reduced-gravity model forced with spatially uniform easterly wind stress of -0.03 N m^{-2}, a value representative of the equatorial zonal average in the Pacific. The thermocline tilts along the equator, being shallow in the east and along the eastern boundary. Sensitivity studies indicate that slight changes in the tilt of the thermocline do not change results qualitatively. To be consistent with the fixed thermocline depth, only the surface Ekman flow, which is generally stronger than the vertical-mean flow in the steady state, is used to advect SST and to compute upwelling velocity. Mechanisms proposed so far for maintaining latitudinal asymmetry in SST, including surface heat flux adjustment (Xie and Philander 1994; Philander et al. 1996) and off-equatorial upwelling (Chang and Philander 1994), are thus retained in this simplified ocean model.

The ocean model spans between 30°S and 30°N. Both current velocity and lateral heat flux are required to vanish on the side boundaries. The model equations are solved by time stepping at a 3° longitude × 1° latitude spatial resolution.

c. Coupling

Only one ocean between 30°S–30°N and 130°E–80°W is set active, whose SST varies according to the model described above. The other ocean basin is used as a reference, whose SST field is held constant in time and zonally uniform. The ocean and atmosphere models exchange information once a day. The atmospheric GCM updates its SST boundary condition daily from the ocean model output and meanwhile passes daily average surface wind stress and heat flux fields to the ocean. The atmospheric wind stress drives ocean Ekman flow and upwelling while surface heat flux directly forces SST. The heat flux at the ocean surface is decomposed into four components:

$$Q = Q_S - Q_L - Q_H - Q_E. \quad (2.3)$$

Here the absorbed solar (Q_S) and net upward longwave (Q_L) radiation is computed with the AGCM's radiation code and varies with the interactive water vapor and cloud fields. The sensible (Q_H) and latent (Q_E) heat fluxes are computed using the AGCM's aerodynamic bulk formulas (Louis 1979; Miller et al. 1992). In particular,

$$Q_E = \rho_a L C_E |\mathbf{U}|[q_s(T) - q_a], \quad (2.4)$$

where ρ_a is the air density, L is the latent heat of water vapor, C_E is the bulk coefficient for evaporation that is a function of wind speed and stability, $\mathbf{U}$ is the wind velocity at 10 m above ground, q_a and q_s are specific humidity of the surface air and that in saturation, respectively. As an important deviation from the original Zebiak–Cane model that treats surface heat flux as a Newtonian damping, Eq. (2.3) incorporates both the WES and cloud–SST feedbacks.

Surface evaporation contains both positive and negative feedbacks on SST. Its temperature dependence is a negative one and can be approximated as a Newtonian cooling with an e-folding time of 1 yr for a 50-m-deep mixed layer (e.g., Xie 1996). Wind-induced evaporation is a positive feedback for equatorially antisymmetric disturbances and may be defined as

$$E_w = \overline{Q}_E(C_E|\mathbf{U}|)'/(\overline{C_E|\mathbf{U}|}), \quad (2.5)$$

where the overbar and prime denote the mean and perturbation, respectively.

Care has been taken in interpolating data between the

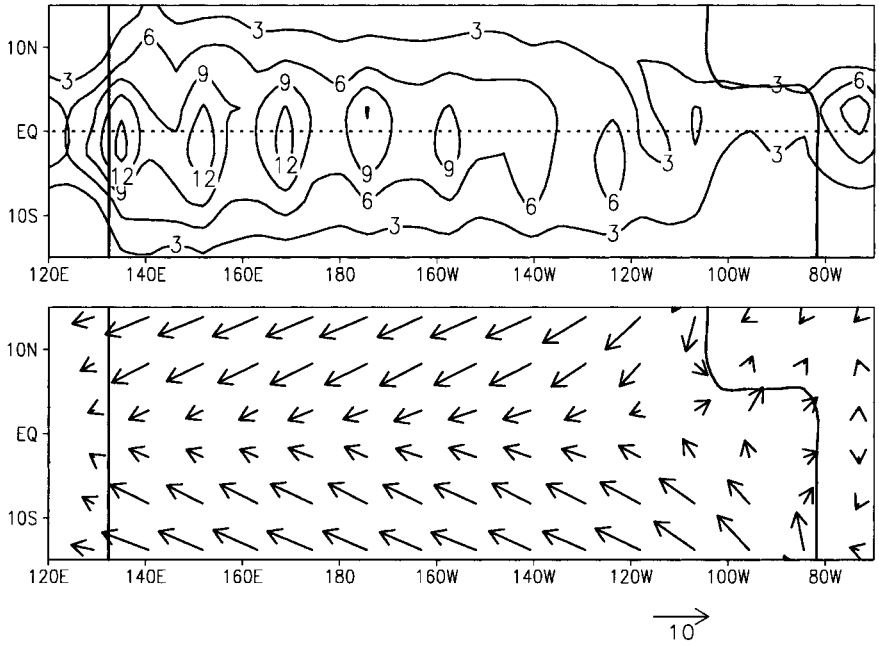

FIG. 3. Precipitation (mm day^{-1}; upper panel) and wind velocity at 985 mb (m s^{-1}; lower) in the stand-alone AGCM run with prescribed SST.

grid points of the ocean and atmosphere models. Given the exchange coefficients in the bulk formulas differ by an order of magnitude between the ocean and land surface, only AGCM outputs on grid points marked as ocean are used in computing momentum and heat flux for the ocean model.

In the control run with all the coastal lines running in a purely meridional direction, the hybrid coupled model settles into a statistically steady state that is symmetric with respect to the equator as expected (more will be said about this control run in section 5). We then add onto the eastern boundary of the active ocean an extra landmass north of the equator to perturb the symmetric climatology. The bulge of landmass is 25° wide in longitude with its southernmost grid point at 8.3°N (Fig. 2). Despite its apparent resemblance to western Africa, we set the active ocean basin to be of the Pacific size. As will be seen, such a large basin size allows the continent-forced asymmetry to fully develop in the zonal direction and thereby helps expose the ocean–atmospheric interaction processes involved far away off the coast. Thus the purpose of this study is not to mimic every detail of the Pacific or the Atlantic climate, but is rather to gain a general understanding of how the coupled ocean–atmosphere system responds to an asymmetric feature on the continent. The ''African'' type continental geometry is chosen because it is perhaps the simplest way to break the equatorial symmetry.

3. Continental forcing

The AGCM is spun up for several years with prescribed SST forcing and the latitudinally symmetric land–sea distribution. Then it is run for another year with the northern bulge of landmass added. After the first three months, the AGCM reaches a new statistically steady state that is displayed in Fig. 3 obtained by averaging the model output for the last nine months. Because the ocean is not yet activated and SST is prescribed symmetric, the model ITCZ is located at the equator onto which surface winds converge.[1] The surface wind field is symmetric about the equator over most of the ocean except near the east end of the basin, where the southerly winds blow across the equator. Despite many differences in model formulation, the Geophysical Fluid Dynamics Laboratory atmospheric GCM simulates a similar response of surface winds to the bulge of northwestern Africa under fixed SST (Philander et al. 1996; Li 1997).

Figure 4a shows a latitude–vertical section of temperature and velocity differences from the control symmetric run averaged between 100° and 90°W, right across the added northern landmass. Replacing the ocean with land surface raises surface temperature as the reduced water supply suppresses evaporation and increases sensible heat flux from the land surface to offset the incident radiative heating. The heated land surface induces intense dry convection that spreads the warming signal to as high as 700 mb. The surface warm-

[1] The wavy feature in the precipitation field is an artifact of spectral truncation that is less pronounced in simulations with realistic SST and masked by large zonal variations in precipitation (A. Numaguti 1999, personal communication).

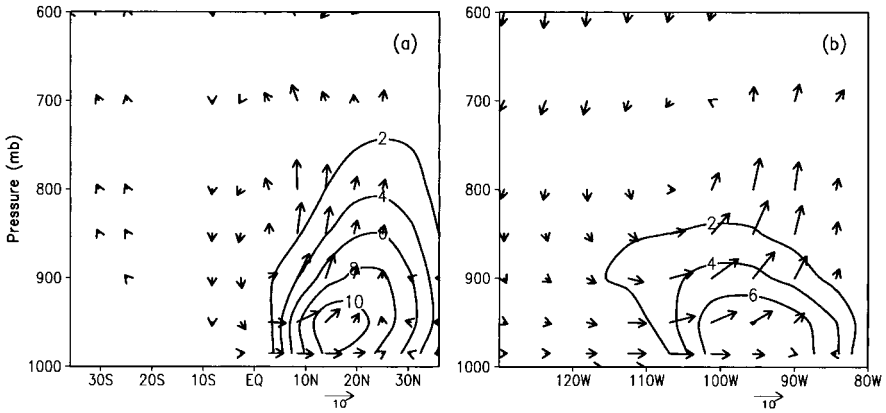

FIG. 4. Temperature (contours; °C) and circulation (vectors; m s^{-1}) anomalies induced by adding a northern bulge to the eastern continent. (a) Meridional section averaged in 100°–90°W, and (b) zonal section at 8.3°N. Vertical velocity is scaled.

ing induces a local sea-breeze-type circulation in the lower atmosphere, with intense rising motion over the northern continent and weak descent south of the equator. The shallow circulation seems to produce a weak equatorial asymmetry in precipitation toward the east end of the basin.

In addition to this meridional cell, the sea breeze has an east–west component (Fig. 4b). Strong anomalous westerly winds flow from the west and converge onto the land bulge. This zonal cell reduces the easterly trades at the surface and hence induces a warming tendency in SST when the ocean is activated. Note that the direct atmospheric response to changes in continental geometry is rather limited in its spatial scale, strongly trapped within a short distance from the coasts (Fig. 5a). In the next section, we allow the ocean to change and examine the effects of these land-induced anomalous winds in the coupled system.

4. Coupled response

a. Transient wave

Upon activating the ocean model, SST anomalies start to develop in the eastern basin (Fig. 5b). On the southeastern boundary the alongshore winds in Fig. 3 induce upwelling and surface cooling. There is a NH counterpart of coastal upwelling cooling barely visible in Fig. 5b. The zonal band of negative SST anomalies immediately south of the equator is a direct effect of off-equatorial upwelling, an oceanic response to southerly cross-equatorial winds (Philander and Pacanowski 1981; Chang and Philander 1994). The warming north of the equator is due to weakened easterly trades that suppress surface evaporative cooling. Although small, there are significant cross-equatorial southerly wind anomalies over the western part of this pair of SST dipole across the equator, which can be readily explained as direct atmospheric response to SST changes.

At $t = 8$ month, the cooling on and south of the equator becomes stronger and extends westward to cover the eastern half of the basin. Both the Bjerknes and the WES feedbacks are responsible. Along the equator, the cooling in the east induces anomalous easterly winds not only locally over cold ocean surface but also remotely over the western basin. Via equatorial upwelling, the enhanced trade winds intensify the cooling and spread it toward the west. Off the equator in the meridional direction, the slight warming to the north and strong cooling to the south of the equator induce anomalous southerly winds. The Coriolis force upon the southerly winds enhances (weakens) the background easterly trade winds (Fig. 3b) south (north) of the equator, acting to increase the north–south SST difference. The anomaly pattern in Fig. 5 may be viewed as a superposition of a symmetric cooling centered on the equator and an antisymmetric seesaw off the equator. This explains why the SST and zonal wind anomalies tend to be small to the north in comparison with those to the south of the equator.

In Fig. 5c, the southeasterly wind anomalies extend much farther westward than the SST anomalies, apparently as a result of atmospheric Rossby waves forced in the east. Wind anomalies in the western basin start to change local SSTs, causing the cooling region to spread farther westward (Fig. 5d). This coupled wind–SST wave substantially reduces precipitation south of the equator while slightly increasing it to the north (Fig. 5e). Whereas SST anomaly decreases in size toward the west, latitudinal asymmetry in precipitation remains strong in the western half of the basin. This nonlinear response of precipitation to SST changes appears to be related to a tendency for equatorial precipitation to increase westward in the AGCM run under zonally uniform SST (Fig. 3a).

In intermediate coupled models or hybrid coupled OGCMs, land surface conditions are usually not treated and assumed to be time invariant. With SST decreasing in the Far East on and south of the equator, precipitation

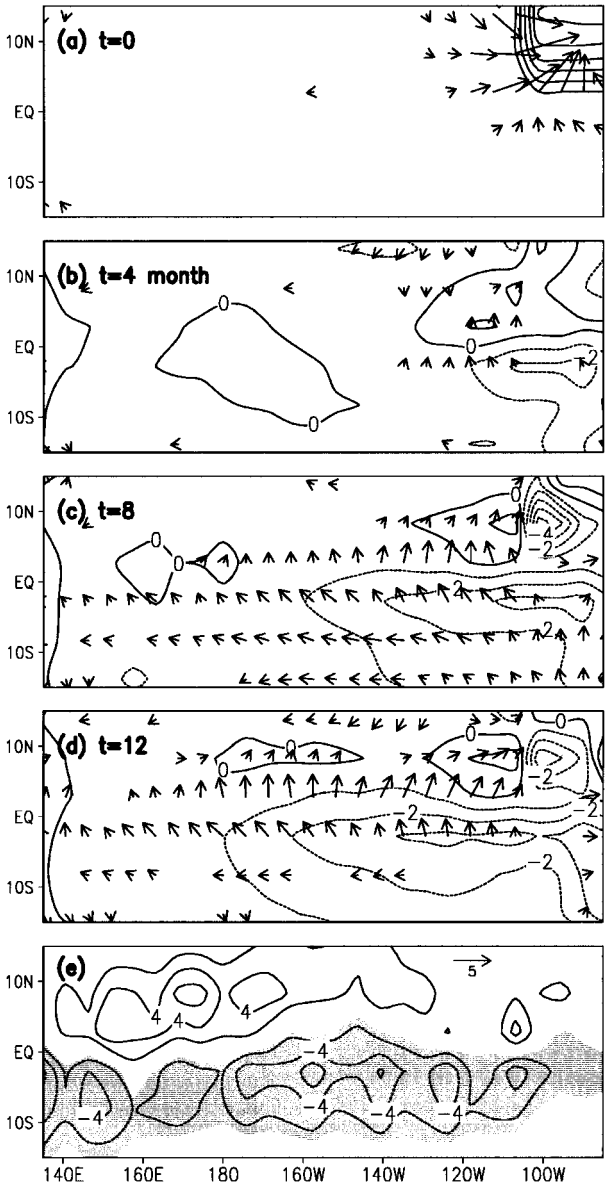

FIG. 5. (a) Atmospheric and (b)–(e) coupled ocean–atmospheric response to a northern bulge on the eastern continent. Vectors are for wind velocity anomalies at 985 mb; contours are for surface temperature anomalies (°C) in (a)–(d) and for precipitation anomalies (mm day^{-1}) in (e). In (a) the anomalies are defined as the difference from the stand-alone symmetric AGCM run, whereas in (b)–(e) they are the differences between the coupled and the asymmetric stand-alone AGCM runs. Thus the atmospheric anomalies in (b)–(e) are solely due to varying SST.

increases slightly over the northern continent, resulting in land surface cooling in the HaGCM with an interactive hydrological cycle. This land surface cooling largely offsets the effect of decreased SST to the south on the sea level pressure, and as a result, the net SST-induced wind anomalies are small south of the land bulge. In this sense, the ground hydrology is a negative feedback in generating the cross-equatorial wind.

The coupled westward propagation is most clearly seen in time–longitude sections. Here we divide near-equatorial anomalies into latitudinally antisymmetric (Figs. 6a,b) and symmetric (Fig. 6c) parts. The cross-equatorial southerlies in the east are a direct response to added landmass to the north. It takes one month for the ocean to establish a northward SST gradient in response to these land-induced southerlies. After about four months, we see a steady westward development of ocean–atmospheric asymmetries characterized by southerly winds and northward SST gradients on the equator. Such coupled development is similar to that in an intermediate model [cf. Fig. 5 with Xie's (1996) Fig. 10] despite more complicated feedbacks in the HaGCM as outlined in section 1. As a major difference, the southerly winds on the eastern boundary, imposed in Xie, are physically induced here by the northern continent bulge.

b. Steady state

The time integration of the hybrid model is continued for nine years. In this section, we discuss the mean state of the hybrid coupled model (Fig. 7), obtained by averaging its outputs for the last five years. Large equatorial asymmetries develop in the SST field, with higher values north of the equator. Accordingly, the model ITCZ shifts to the north of the equator, onto which the surface winds converge. Beneath the northerly ITCZ, winds are weak in contrast to strong southeasterly winds on the other side of the equator. Because of the coarse resolution of the AGCM, the northward departure of the model ITCZ is less pronounced than in observed annual-mean climatology.

We now consider what maintains the climatic asymmetry over the ocean away from the continents, by examining profiles of model quantities averaged between 140° and 120°W (Fig. 8). We will focus on the differences on the two sides of the equator (Table 1). The WES feedback is at work. Although latent heat flux is about the same in the two latitude bands, evaporation efficiency ($C_E|\mathbf{U}|$) is 20% smaller in the northern than the southern band. This evaporation efficiency is mainly controlled by the mean wind velocity while transient winds also play a role, particularly beneath the ITCZ where winds are highly variable. The weak mean wind velocity at 2.8°N is a direct consequence of local wind convergence (Fig. 8, the second from the top), which is in turn controlled by SST distribution. In addition to the WES contribution, low-level clouds tend to form over the cold ocean surface south of the equator in the model. As a result, solar radiation at 8.3°S falls slightly below that at 8.3°N despite abundant deep clouds in the NH ITCZ.

The bottom panel of Fig. 8 shows the meridional and vertical advection terms, whose sum balances the net surface heat flux. In response to southerly winds, strong asymmetry develops in upwelling, displacing the SST minimum slightly south of the equator. Since the up-

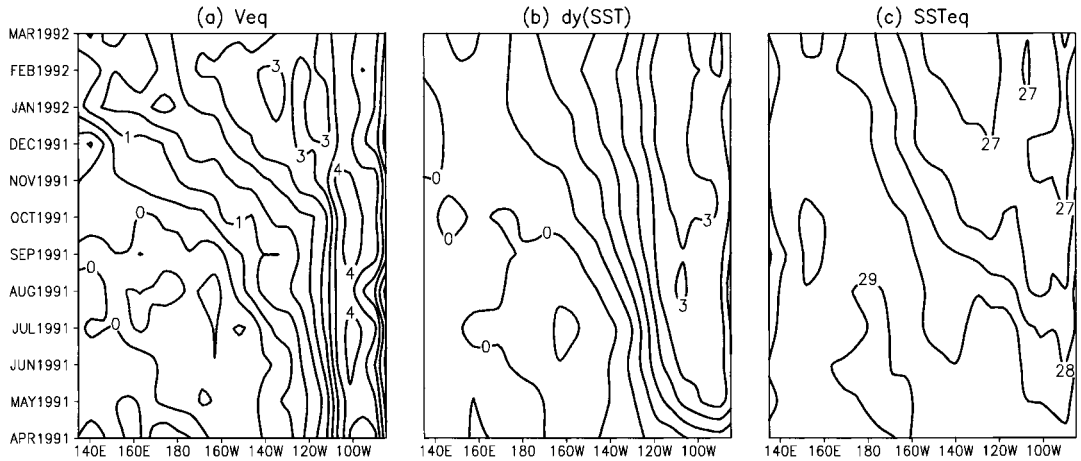

FIG. 6. Latitude–time sections of (a) cross-equatorial wind velocity (m s^{-1}), (b) SST difference (°C) between 2.8°N and 2.8°S, and (c) equatorial SST averaged between 2.8°N–S in the coupled run. The asymmetric AGCM run with fixed SST is used to initialize the coupled run.

welling is confined within a narrow zone, its direct effect is small off the equator; SST is 28.8°C (27.3°C) while upwelling cooling is 11 (13) W m^{-2} at the northern (southern) SST maximum. The difference in wind-induced latent heat flux [Eq. (2.5)] between the two latitudes, by contrast, is about 25 W m^{-2}. The upwelling has an indirect influence on off-equatorial SST maxima by changing their latitudes. On the eastern boundary at 15°S, upwelling cooling is quite intense at 50 W m^{-2} while insolation is 60 W m^{-2} lower than in the interior ocean to the west. This coastal upwelling, along with dense low-level clouds off the coast, helps to initiate the westward development of coupled asymmetries. Thus, the WES, stratus–SST, and upwelling–SST feedbacks act cooperatively in moving the ITCZ to the north of the equator. In a different hybrid coupled GCM, Li (1997) reaches a similar conclusion with regard to relative importance of these feedbacks.

Figure 9 shows zonal profiles of meridional wind velocity, which may be taken as a measure of equatorial asymmetry. Since meridional wind fluctuations have a standard deviation of about 0.5 m s^{-1} (see section 5), the cross-equatorial wind velocity is significantly positive for the coupled run. In the stand-alone AGCM run

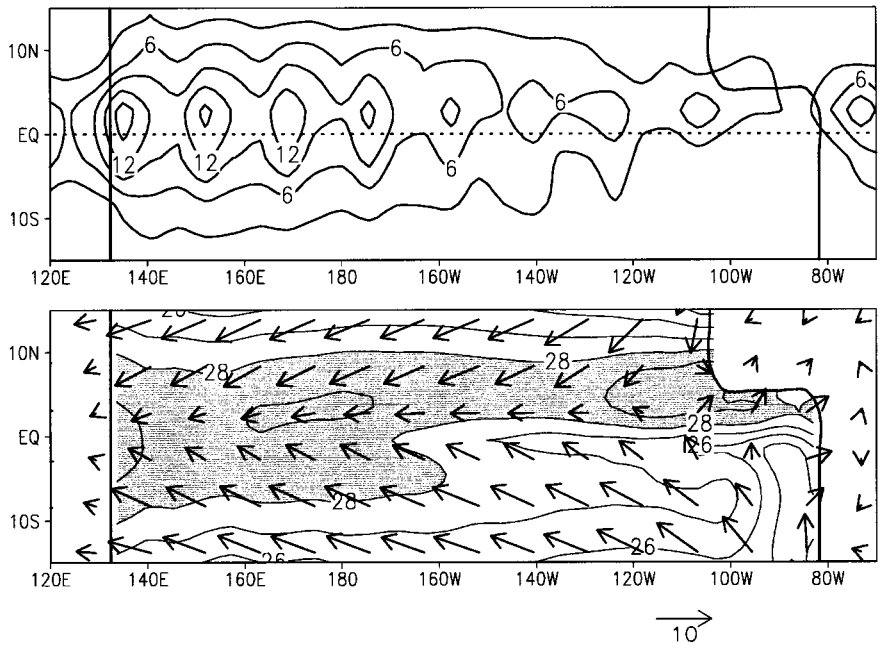

FIG. 7. Mean state of the coupled run: 5-yr average precipitation (mm day^{-1}; upper panel), SST (°C), and surface wind velocity (m s^{-1}; lower).

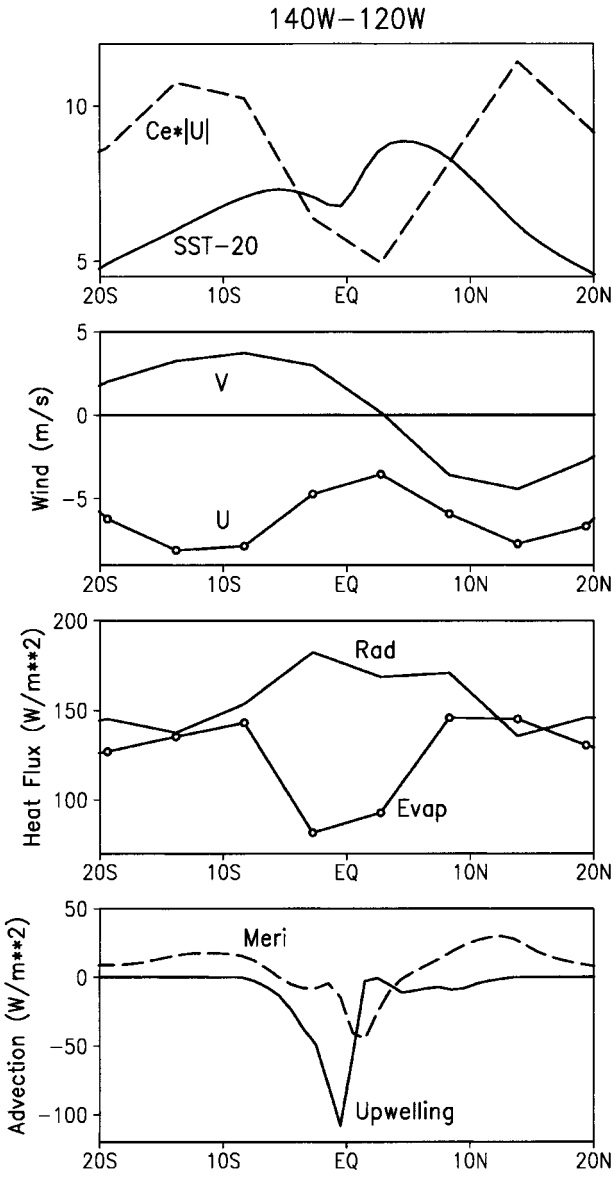

FIG. 8. From the top panel: meridional distributions of 140°–120°W average SST (offset by 20°C) and evaporation efficiency (10^{-3} m s^{-1}); zonal (U) and meridional (V) wind velocities; net downward radiation and latent heat flux at the sea surface; and vertical and meridional advection by ocean currents in the coupled run.

with prescribed symmetric SST, the cross-equatorial winds are confined to longitudes immediately south of the continent bulge and indistinguishable from vanishing west of 130°W. Only with the help of SST asymmetries, does asymmetric atmospheric circulation develop into a basinwide structure. In a simple model, the zonal profile of cross-equatorial wind is determined by the growth character of the coupled wave (Xie 1996). A positive (negative) temporal growth rate leads to a westward increase (decrease) of latitudinal asymmetry in the steady state.

TABLE 1. Cross-equatorial comparison of SST, net downward radiation (R), evaporation (E), evaporation efficiency ($C_E|\mathbf{U}|$), and zonal (U) and meridional (V) wind velocities, averaged in 140°–120°W and 2.8°–8.7°N–S.

	T (°C)	R (W m^{-2})	E (W m^{-2})	$C_E\|\mathbf{U}\|$ (10^{-3} m s^{-1})	U (m s^{-1})	V (m s^{-1})
N	28.4	170	119	6.6	−4.7	−1.7
S	27.1	168	112	8.3	−6.3	3.3

c. Westward control by the continent

Up to this point, we have focused on a case with the continent bulge located on the eastern boundary of the active ocean basin. Now we turn our attention to a contrasting case where the bulge of landmass is moved to the western boundary (Fig. 10b). Any asymmetric response of the atmosphere to this continental forcing has to take the form of the Rossby wave and therefore is confined to the west of the continental forcing. As a result, the ocean–atmosphere system to the east does not know a symmetry-breaking landmass has been added to the western boundary and stays in a statistically sym-

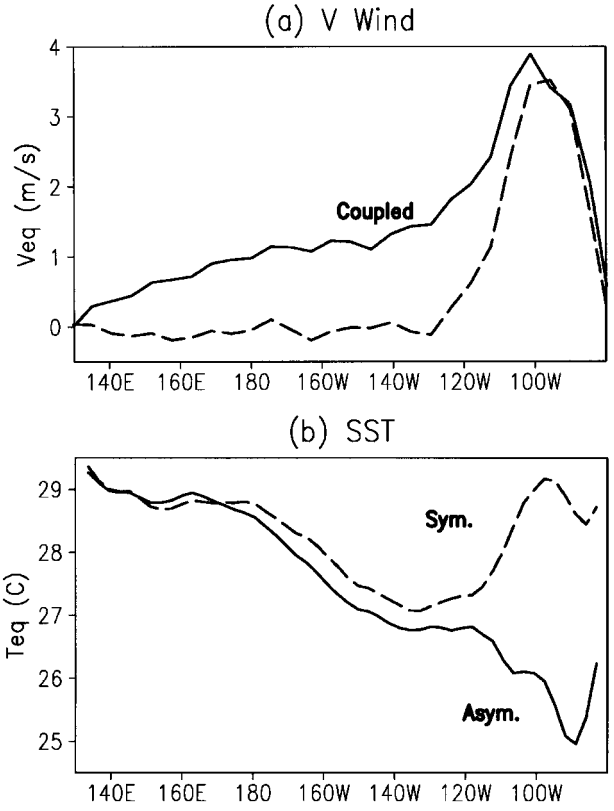

FIG. 9. Zonal distributions of (a) cross-equatorial wind velocity in the stand-alone AGCM (dashed) and coupled (solid) runs and (b) SST at the equator in the symmetric (dashed) and at 1°S in the asymmetric (solid) coupled runs. In the asymmetric run, the center of the equatorial cold tongue shifts slightly south of the equator because of the upwelling induced by cross-equatorial southerly winds.

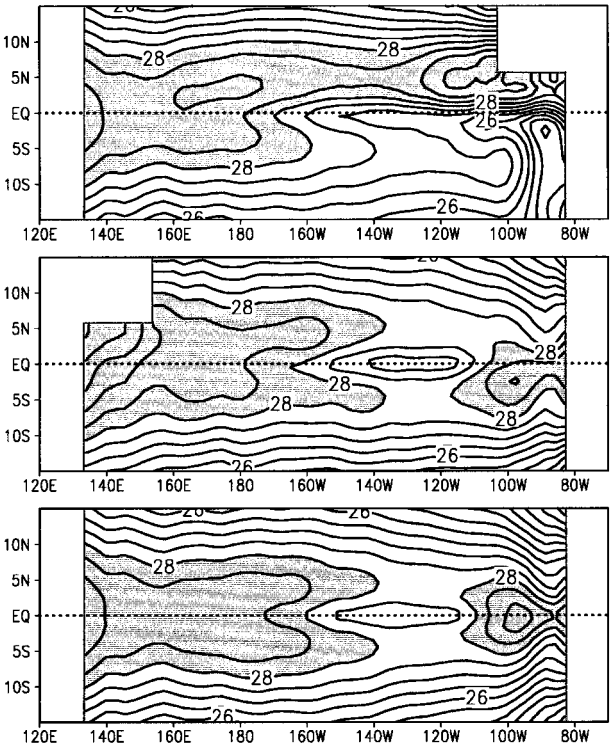

FIG. 10. Time–mean SST (>28°C shaded) distributions in coupled runs with a northern bulge on (a) the eastern and (b) western continent and (c) with continents perfectly symmetric about the equator.

metric state. Weak asymmetries in SST develop at longitudes immediately south of the continent bulge. East of 155°E, the steady-state solution under the western continental forcing is not significantly different from that under perfectly symmetric boundary conditions (Fig. 10c). This thus demonstrates that the continental forcing exerts a one-way control over the climatology of the coupled system to the west. The experiment further suggests that the hemispheric difference in area of landmass—a favorite forcing candidate for global control hypotheses—is less important than the continental geometry on the eastern boundary.

West of 50°W, the north coast of South America is located south of the equator, a land–sea distribution resembling Fig. 10b albeit with the north and south reversed. This contrast between a landmass to the south and ocean to the north induces northerly winds across the equator, a latitudinal asymmetry that would favor a southern ITCZ. Thus, the Atlantic ITCZ appears to involve a competition between Africa to the east and South America to the west. The African continent obviously wins the competition, moving the Atlantic ITCZ to the north of the equator. Because of the small zonal size of the ocean, the effects of South America on the Atlantic cannot be ruled out and need further investigation.

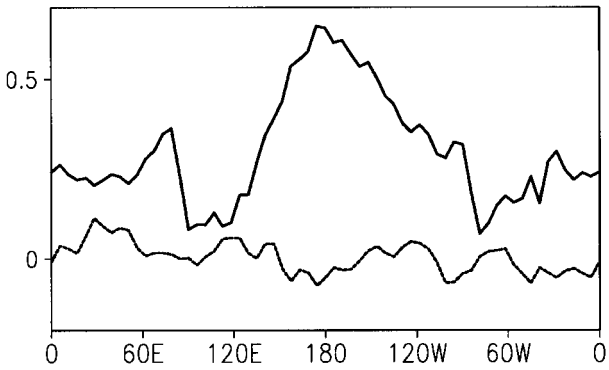

FIG. 11. Time average (lower curve) and variance (upper curve) of cross-equatorial wind velocity (m s^{-1}) in the symmetric coupled run. The variance is computed using the 3-month running means.

d. Effects on the equatorial cold tongue

The development of latitudinal asymmetry has a further consequence to the zonal structure of the equatorial cold tongue, as revealed by a comparison of Fig. 10's three panels. In the far eastern ocean, zonal winds are westerly converging onto the continent in all three cases much as in Fig. 7b. This prevents the equatorial upwelling from occurring. The eastern cooling in the asymmetric run with an eastern continental forcing is caused by cross-equatorial winds through upwelling both on the coast and south of the equator. This southerly wind-induced cooling mechanism is important for the real Pacific Ocean where the zonal winds near the surface are blocked by the Andes and vanish on the American coasts (Xie 1998). Figure 9b contrasts the equatorial cold tongues between the symmetric and asymmetric runs. SSTs decrease by as much as 3°C in the east in the asymmetric run. The cooling extends farther westward of the continent bulge due to the Bjerknes feedback: the eastern cooling enhances easterly trades to the west that induce further cooling via equatorial upwelling, much as in Fig. 6c.

5. Temporal variability

The atmosphere contains internal variability independent of SST, which may interact with the ocean and excite particular coupled modes (Chang et al. 1997; Xie 1999). Even under latitudinal symmetric continental geometry, the hybrid coupled model displays substantial asymmetries at a given time. As a measure of latitudinal asymmetry, we display in Fig. 11 root-mean-square variance of low-frequency (timescale $>$ 3 months) variability for near-surface meridional wind velocity on the equator. The variance reaches minimum over continent presumably because of large surface drag. The ocean–atmosphere coupling apparently enhances the amplitude of latitudinal asymmetric disturbances over the active ocean by a factor of 2 as compared with that over the inactive ocean where the SST is kept time invariant.

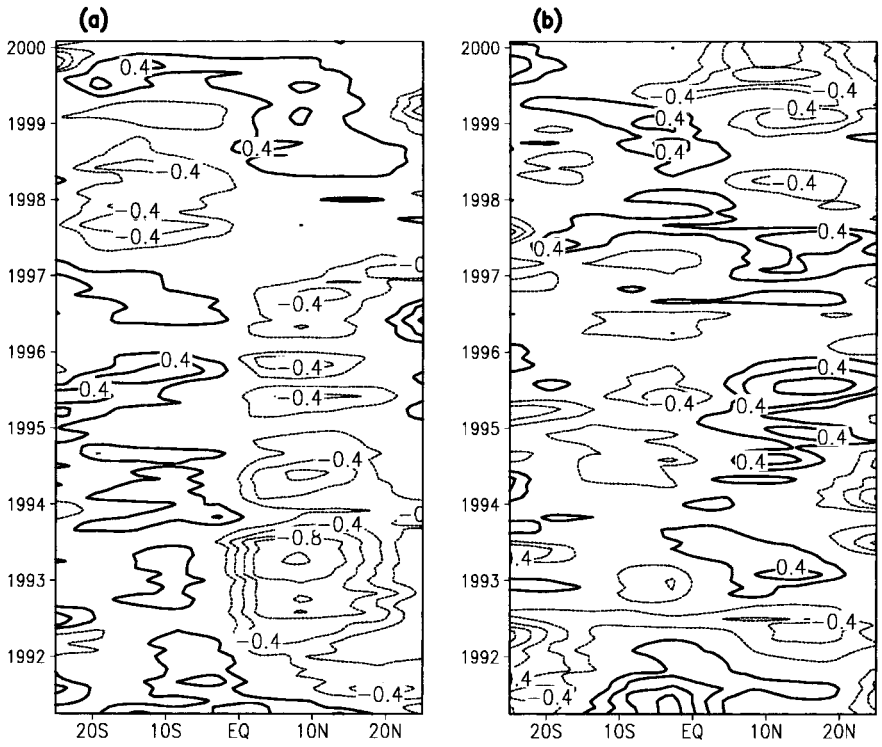

FIG. 12. Latitude–time sections of SST anomalies (180°–140°W average) in (a) the symmetric and (b) asymmetric coupled runs.

SST variability is key to the enhanced variance in cross-equatorial wind over the active ocean basin. Figure 12 shows the latitude–time section of SST anomaly in the midbasin. SST displays interannual variations that may be characterized as a north–south seesaw across the equator with a typical amplitude of 0.5°C. We examine the meridional structure of the coupled mode by correlating model fields with interhemispheric SST difference between 7°–14°N–S (Fig. 13). The SST pattern is dipolar with two opposing poles located around 10°–15° latitude and is associated with north–southward shift in the equatorial ITCZ. The SST dipole forces significant cross-equatorial winds that induce zonal wind anomalies that are positively correlated with SST anomalies. All this indicates that the coupled WES feedback is involved in causing the meridional dipole oscillation in the hybrid model.

Figure 14a shows the horizontal distribution of the correlation with an index of the north–south seesaw variability. The wind pattern, with enhanced (weakened) easterly trades south (north) of the equator, and the associated evaporation anomaly pattern acts to reinforce the existing SST anomaly against the Newtonian thermal damping. The coupled anomalies are nearly zonally uniform, consistent with the linear theory that the WES waves attain the maximum growth rate at zero zonal wavenumber (Xie 1996).

Weak but significant changes in cloud cover are associated with the dipole SST oscillation. Figure 14b shows the correlation map of downward solar radiation at the sea surface. Changes in deep convective clouds are responsible for the near-equatorial cloud dipole within 5°N–S with more clouds on the warmer side of the equator—a negative feedback. The seesaw poleward of 5°N–S, on the other hand, involves shallow clouds in the model PBL, with less clouds over a warm SST anomaly—a positive feedback. In this symmetric run, precipitation is heavily concentrated on the equator. Stratiform clouds form in the PBL immediately poleward of the equatorial ITCZ, and the mean low-level cloud cover reaches a maximum at 15°N–S (not shown). The maximum cloud variability associated with the SST dipole coincides with these boundary layer stratiform cloud bands off the equator. Such an association between the SST dipole and a cloudiness quadripole is observed in the real tropical Atlantic (Fig. 14, right panels). As in the model, high and low clouds respond to local SST changes in opposing ways.

Figure 13c shows the regressions of wind-induced evaporation [E_w in Eq. (2.5)], upwelling, and solar radiation anomalies based on the SST dipole index. A positive contributor to the SST dipole, anomalous upwelling is strongly equatorially trapped and nearly offsets the negative effect of deep-cloud variability associated with the ITCZ. In the dipole's centers of action, both the WES and shallow cloud–SST feedbacks are important, with the former being twice as large in amplitude. Anomalous shallow clouds are nearly in phase

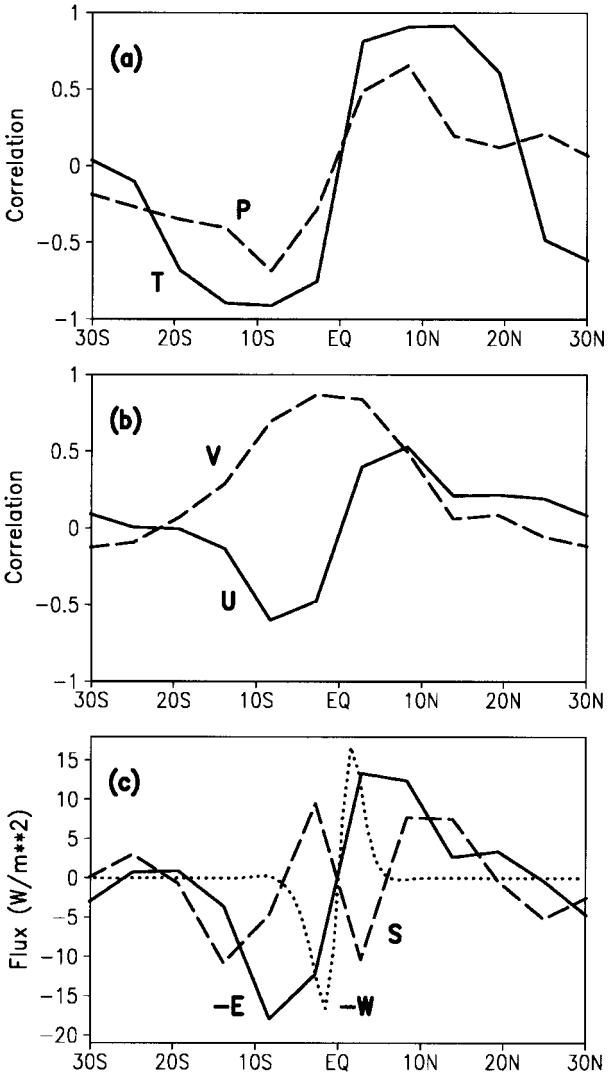

FIG. 13. Correlation coefficients with interhemispheric SST difference between 8.3°–13.8°N–S: (a) SST, precipitation (dashed) and (b) zonal and meridional (dashed) wind velocities. (c) Regressions for upwelling (W), solar radiation (S) and wind-induced evaporation (E) fluxes (W m^{-2} K^{-1}) onto the interhemispheric SST difference. All are for 180°–140°W averages.

with local SST anomalies and their effects may be viewed as reducing the Newtonian damping rate. Based on an analysis of tropical Atlantic dipole, Tanimoto and Xie (2000) estimate that the reduction is about 20%–30% of the rate arising from the SST dependence of surface evaporation.

It is worth noting that the phase of zonal wind/wind-induced evaporation shifts slightly equatorward of the SST's, which would cause the coupled anomalies to move equatorward. The simple model results (Xie 1999) suggests that the poleward oceanic Ekman flow induced by the mean easterly winds is critical to stopping this potential equatorward phase propagation and giving rise to the quasi-stationarity of the WES mode in the meridional direction. Indeed, the dipolar oscillation displays such a tendency for equatorward phase propagation in an AGCM coupled with a one-dimensional mixed layer (D. Battisti and E. Sarachik 1999, personal communication).

Similar dipole oscillation is seen in the asymmetric run where the bulge on the eastern continent pushes the climatological ITCZ into the Northern Hemisphere (Fig. 12b). As compared with the symmetric run, the nodal point of the SST dipole appears to shift slightly northward. With a northward displaced ITCZ in the mean state, anomalous southerly winds associated with the dipole mode cool equatorial SST by enhancing surface evaporation and upwelling. In contrast to the formation of the mean climate where continental asymmetry is the key forcing, the SST dipole does not seem significantly correlated with either precipitation or surface temperature on the northern land bulge (not shown).

6. Discussion

A hybrid coupled GCM is developed to study the processes driving the tropical climate away from the equatorial symmetry that the annual-mean solar radiation would otherwise force. It consists of an intermediate ocean model and an atmospheric GCM with interactive ground hydrology and interactive cloud-radiation packages. The model is designed to include all the major mechanisms proposed for causing latitudinal asymmetry in SST. Specifically, the model SST is forced by surface heat flux and advected three-dimensionally by a flow field based on Ekman dynamics. The simplicity of the ocean has facilitated our comparison and interpretation with previous theoretical studies.

The continents in the control run are perfectly symmetric relative to the equator with straight meridional coastal lines. Our continental forcing to perturb the symmetric climate is a northern bulge of landmass 25° wide in longitude with the south coast at 5°N. A westward control mechanism implied by linear wave dynamics is explicitly demonstrated by comparing the model response to an eastern and western continental forcing. Basinwide climatic asymmetry develops only when the land bulge is added onto the eastern continent, whereas equatorial symmetry remains over most of the oceanic basin when the same continental forcing is applied to the west. This supports the linear wave dynamics argument that the westward control arises because both the atmospheric Rossby waves directly forced by the land bulge and the coupled WES waves allow only one-way information propagation toward the west. The direct atmospheric response to the addition of the continent bulge is rather coastally trapped, with a limited range of influence in both the zonal and meridional directions. Upon activating the ocean model, a coupled ocean–atmospheric wave front emits from the east and propagates westward, lowering SSTs on and south of the equator and displacing the ITCZ into the Northern

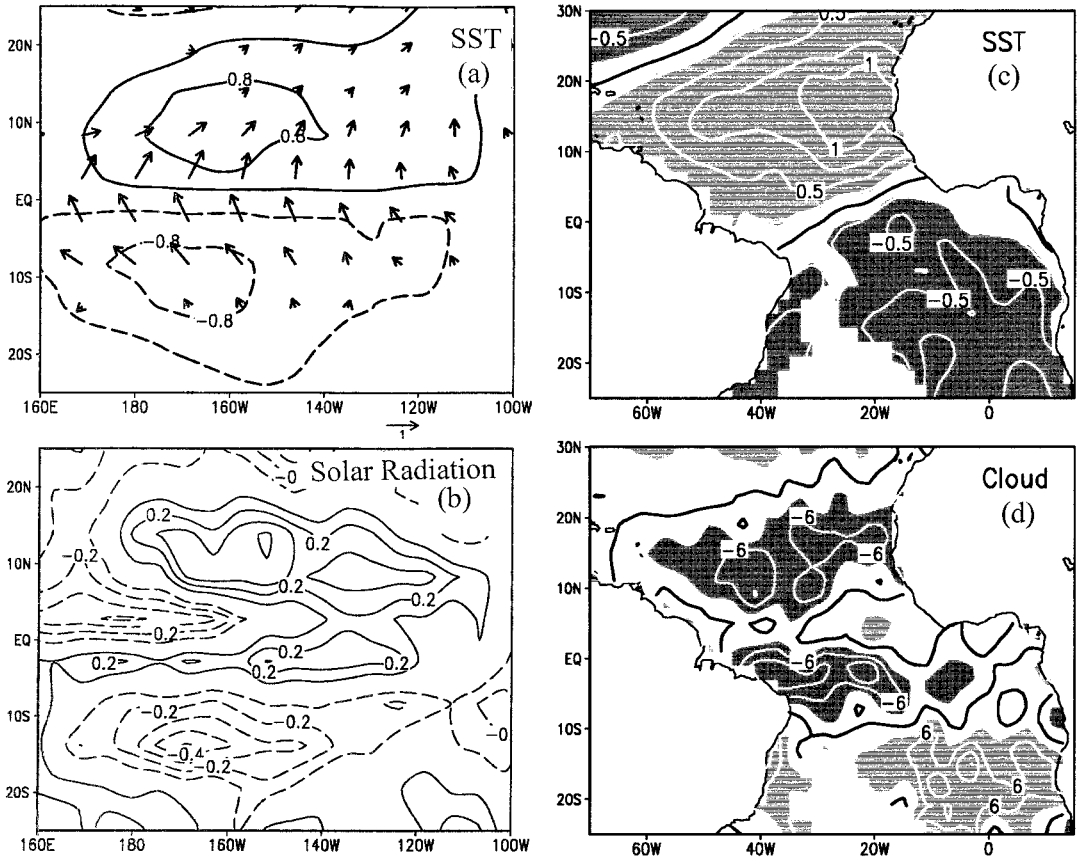

FIG. 14. Correlation coefficients with 180°–140°W mean interhemispheric SST gradient in the symmetric coupled run: (a) SST (contours), wind velocity (vectors), and (b) downward solar radiation at the sea surface. Observed differences between six years of high (1968–70, 1979–81) and low (1972–74, 1984–86) cross-equatorial SST gradient over the tropical Atlantic: (c) SST (°C) and (d) cloudiness (%). The Feb–Apr mean Comprehensive Ocean–Atmosphere Data Sets data are used.

Hemisphere. A number of CGCMs appear to show similar remote response to an asymmetric stratus-cloud forcing off the Peruvian coast (Philander et al. 1996; Ma et al. 1996; Kimoto and Shen 1997; Iizuka et al. 1998; Yu and Mechoso 1999), suggesting that the westward control may indeed be a robust mechanism of the coupled system.

The AGCM allows us to isolate and study the continental forcing in details, including what is the direct atmospheric response to an asymmetric continental feature and how it triggers ocean–atmospheric feedback. Besides the cross-equatorial southerlies noted in previous studies, the zonal sea-breeze circulation induced by the northern bulge of land is identified as an additional symmetry-breaking force that weakens the surface easterly winds and thereby raises the SST off the coast of the northern land bulge. A number of feedback mechanisms not included in the intermediate model of Xie (1996) are found to operate in the HaGCM. Among them is the cloud–SST feedback. This HaGCM is found to be able to simulate both the negative deep-cloud and positive shallow-cloud feedbacks on SST. This difference in response between these different types of clouds is best illustrated in the model dipole oscillation (Fig. 14). In addition, variable winds associated with ITCZ convection and ground hydrology over the land bulge are found to be negative feedbacks in the development of latitudinal asymmetry. In support of Li (1997), the WES, shallow cloud–SST and upwelling–SST feedbacks are the three major mechanisms that positively contribute to the northward displacement of the ITCZ. While it may not directly affect heat budget at off-equatorial SST maxima, upwelling helps initiate climatic asymmetry by cooling the coastal ocean to the south of the equator.

The prevailing easterly trade winds establish a zonal tilt of the thermocline and set the larger stage for ocean–atmosphere interaction in the equatorial Pacific. With the shallow thermocline, the eastern Pacific is favored for developing various coupled instabilities, both symmetric and antisymmetric. This explains why the largest departures from both the zonal and latitudinal symmetry are found in the east. The large anomalies in the east do not necessarily imply that their forcing must come

from the east. In fact, symmetric perturbations—such as equatorial zonal wind—in the west will generate the Kelvin wave and lead to marked changes in equatorial SSTs in the east. The equatorial symmetric ENSO is such an example (Neelin et al. 1998). An equatorially antisymmetric perturbation—such as cross-equatorial wind—in the west, by contrast, has little effect on the east as is demonstrated by our HaGCM experiments.

Under steady solar forcing, the model ITCZ displays temporal variability around a stastically steady state. The interaction with the ocean is found to increase the variability in cross-equatorial wind by a factor of 2. A coupled dipole mode is found to be responsible for the ITCZ variability in the model, with SST varying in opposite polarities across the equator. Both the WES and cloud–SST feedbacks are shown to be involved in this interhemispheric mode of variability. Particularly, the coupled SST dipole and cloud quadripole patterns in the model resemble those observed in the tropical Atlantic (Fig. 14). The existence of a coupled dipole mode in the HaGCM is encouraging, given the controversy over whether the atmospheric response to a dipole SST pattern provides a positive feedback (Chang et al. 2000; Sutton et al. 2000). Our results indicate that the cloud effects need to be taken into account in evaluating atmospheric feedback.

The dominance of the dipole mode in the model, however, may be an artifact of prescribing thermocline depth. The inclusion of the thermocline feedback will enhance the equatorially symmetric variability and even lead to self-sustaining ENSO in a large ocean basin. The linear interference and nonlinear interaction of the symmetric and the dipole modes will complicate the variability that emerges as in the tropical Atlantic. In forming the mean state, an interactive thermocline will certainly affect the equatorial cold tongue, which may modify the strength of ocean–atmospheric feedbacks and hence the configuration of the ITCZ. As the ITCZ shifts into the Northern Hemisphere, the thermocline depth will develop its own equatorial asymmetry, an effect that acts to enhance the upwelling feedback on SST and may be important particularly off the eastern boundary. The effects of this thermocline feedback on the ITCZ and its variability need to be studied in the future.

The African-type land bulge is used in this study to perturb an otherwise symmetric system. The simplicity of this continental forcing allows us to focus on the initiation and westward development of coupled asymmetries in the ocean and atmosphere. When applied to the Pacific ocean–atmospheric system, the westward control mechanism implies that the forcing for the perennial NH ITCZ is likely on the American continents in the east rather than on Eurasia in the west. There are many asymmetric features on the American continents that can affect latitudinal asymmetry of the Pacific climate. Like Africa, Central America is located west of South America but has much smaller landmass. The northwestward slanted coastline can favor a NH ITCZ via the initiation of coastal upwelling (Philander et al. 1996; Li 1997). It is unclear what roles the narrow and steep Andes play, which are poorly represented in GCMs. Despite the recent progress in our understanding of coupled nature of the Pacific ITCZ, it remains a challenge to keep it north of the equator in fully coupled GCMs. How each of these asymmetric features on the Americas affects the Pacific to the west and how they collectively initiate climatic asymmetry await further investigations.

Acknowledgments. We would like to thank A. Numaguti and N. Saiki for assistance in developing the coupled model; M. Kimoto, D. Battisti, and E. Sarachik for helpful discussions; W. T. Liu for providing the QuikSCAT wind data; H. Okajima for skillfully handling the model data; and anonymous referees for constructive comments. Supported by grants from CCSR/University of Tokyo, the Ministry of Education and the Asahi Breweries Foundation for the Promotion of Science. The IPRC is partly supported by the Frontier Research System for Global Change.

REFERENCES

Arakawa, A., and W. H. Schubert, 1974: Interactions of cumulus cloud ensemble with large-scale environment. *J. Atmos. Sci.,* **31,** 671–701.

Bjerknes, J., 1969: Atmospheric teleconnections from the equatorial Pacific. *Mon. Wea. Rev.,* **97,** 163–172.

Carton, J., X. Cao, B. S. Giese, and A. M. da Silva, 1996: Decadal and interannual SST variability in the tropical Atlantic Ocean. *J. Phys. Oceanogr.,* **26,** 1165–1175.

Chang, P., and S. G. H. Philander, 1994: A coupled ocean–atmosphere instability of relevance to the seasonal cycle. *J. Atmos. Sci.,* **51,** 3627–3648.

——, L. Ji, and H. Li, 1997: A decadal climate variation in the tropical Atlantic Ocean from thermodynamic air–sea interactions. *Nature,* **385,** 516–518.

——, R. Saravanan, L. Ji, and G. C. Hegerl, 2000: The effects of local sea surface temperatures on atmospheric circulation over the tropical Atlantic sector. *J. Climate,* **13,** 2195–2216.

Dijkstra, H. A., and J. D. Neelin, 1995: Ocean–atmosphere interaction and the tropical climatology. Part II: Why the Pacific cold tongue is in the east. *J. Climate,* **8,** 1343–1359.

Enfield, D. B., A. M. Mestas-Nunez, D. A. Mayer, and L. Cid-Serrano, 1999: How ubiquitous is the dipole relationship in tropical Atlantic sea surface temperatures? *J. Geophys. Res.,* **104,** 7841–7848.

Esbensen, S. K., and M. J. McPhaden, 1996: Enhancement of tropical ocean evaporation and sensible heat flux by atmospheric mesoscale systems. *J. Climate,* **9,** 2307–2325.

Gill, A. E., 1980: Some simple solutions for heat-induced tropical circulation. *Quart. J. Roy. Meteor. Soc.,* **106,** 447–462.

Iizuka, S., T. Matsuura, M. Chiba, and M. Sugi, 1998: A sensitivity experiment of a coupled ocean–atmosphere GCM: Impacts of marine stratus on sea surface temperatures. *Rep. Nat. Res. Inst. Earth Sci. Disaster Prev.,* **58,** 53–60.

Kimoto, M., and X. Shen, 1997: Climate variability studies using general circulation models. *The Frontiers of Climate Research II,* S. Sumi, Ed., CCSR/University of Tokyo, 91–116.

Le Treut, H., and Z. X. Li, 1991: Sensitivity of an atmospheric general circulation model to prescribed SST changes: Feedback effects associated with the simulation of cloud optical properties. *Climate Dyn.,* **5,** 175–187.

Li, T., 1997: Air–sea interactions of relevance to the ITCZ: Analysis of coupled instabilities and experiments in the hybrid coupled GCM. *J. Atmos. Sci.,* **54,** 134–147.

——, and T. F. Hogan, 1999: The role of the annual-mean climate on seasonal and interannual variability of the tropical Pacific in a coupled GCM. *J. Climate,* **12,** 780–792.

Liu, W. T., X. Xie, P. S. Polito, S.-P. Xie, and H. Hashizume, 2000: Atmospheric manifestation of tropical instability waves observed by QuikSCAT and Tropical Rainfall Measuring Mission. *Geophys. Res. Lett.,* **27,** 2545–2548.

Louis, J., 1979: A parameteric model of vertical eddy fluxes in the atmosphere. *Bound.-Layer Meteor.,* **17,** 187–202.

Ma, C.-C., C. R. Mechoso, A. W. Robertson, and A. Arakawa, 1996: Peruvian stratus clouds and the tropical Pacific circulation—A coupled ocean–atmosphere GCM study. *J. Climate,* **9,** 1635–1645.

Manabe, S., J. Smagorinski, and R. F. Strickler, 1965: Simulated climatology of a general circulation model with a hydrologic cycle. *Mon. Wea. Rev.,* **93,** 769–798.

Matsuno, T., 1966: Quasi-geostrophic motions in the equatorial area. *J. Meteor. Soc. Japan,* **44,** 25–43.

Mechoso, C. R., and Coauthors, 1995: The seasonal cycle over the tropical Pacific in coupled ocean–atmosphere general circulation models. *Mon. Wea. Rev.,* **123,** 2825–2838.

Miller, G. L., A. C. M. Beljaars, and T. N. Palmer, 1992: The sensitivity of the ECMWF model to the parameterization of evaporation from the tropical oceans. *J. Climate,* **5,** 418–434.

Mitchell, T. P., and J. M. Wallace, 1992: The annual cycle in equatorial convection and sea surface temperature. *J. Climate,* **5,** 1140–1156.

Nakajima, T., and M. Tanaka, 1986: Matrix formulation for the transfer of solar radiation in a plane-parallel scattering atmosphere. *J. Quant. Spectrosc. Radiat. Transfer,* **35,** 13–21.

Neelin, J. D., D. S. Battisti, A. C. Hirst, F. F. Jin, Y. Wakata, T. Yamagata, and S. Zebiak, 1998: ENSO theory. *J. Geophys. Res.,* **103,** 14 261–14 290.

Nobre, P., and J. Shukla, 1996: Variations of sea surface temperature, wind stress, and rainfall over the tropical Atlantic and South America. *J. Climate,* **9,** 2464–2479.

Numaguti, A., 1999: Origin and recycling processes of precipitating water over the Eurasian continent: Experiments using an atmospheric general circulation model. *J. Geophys. Res.,* **104,** 1957–1972.

——, M. Takahashi, T. Nakajima, and A. Sumi, 1997: Description of CCSR/NIES atmospheric general circulation model. *CGER Supercomputer Monogr. Report,* No. 3, National Institute for Environmental Studies, 1–48.

Philander, S. G. H., and R. C. Pacanowski, 1981: Oceanic response to cross-equatorial winds with application to coastal upwelling in low latitudes. *Tellus,* **33,** 201–210.

——, D. Gu, D. Halpern, G. Lambert, N.-C. Lau, T. Li, and R. C. Pacanowski, 1996: The role of low-level stratus clouds in keeping the ITCZ mostly north of the equator. *J. Climate,* **9,** 2958–2972.

Sun, D.-Z., and Z. Liu, 1996: Dynamic ocean–atmosphere coupling: A thermostat for the tropics. *Science,* **272,** 1148–1150.

Sutton, R. T., S. P. Jewson, and D. P. Rowell, 2000: The elements of climate variability in the tropical Atlantic region. *J. Climate,* **13,** 3261–3284.

Tanimoto, Y., and S.-P. Xie, 2000: Inter-hemispheric decadal variations in SST, surface wind and heat flux over the Atlantic basin. Japan Marine Sci. and Technol. Center Rep. No. 41, 57–68.

Terray, L., 1998: Sensitivity of climate drift to atmospheric physical parameterizations in a coupled ocean–atmosphere general circulation model. *J. Climate,* **11,** 1633–1658.

Xie, S.-P., 1996: Westward propagation of latitudinally asymmetry in a coupled ocean–atmosphere model. *J. Atmos. Sci.,* **53,** 3236–3250.

——, 1998: Ocean–atmosphere interaction in the making of the Walker circulation and the equatorial cold tongue. *J. Climate,* **11,** 189–201.

——, 1999: A dynamic ocean–atmosphere model of the tropical Atlantic decadal variability. *J. Climate,* **12,** 64–70.

——, and S. G. H. Philander, 1994: A coupled ocean–atmosphere model of relevance to the ITCZ in the eastern Pacific. *Tellus,* **46A,** 340–350.

Yu, J.-Y., and C. R. Mechoso, 1999: Links between annual variations of Peruvian stratocumulus clouds and of SST in the eastern equatorial Pacific. *J. Climate,* **12,** 3305–3318.

Zebiak, S. E., 1982: A simple atmosphere model of relevance to El Niño. *Mon. Wea. Rev.,* **110,** 1263–1271.

——, and M. A. Cane, 1987: A model El Niño–Southern Oscillation. *Mon. Wea. Rev.,* **115,** 2262–2278.